Hindawi
Journal of Sensors
Volume 2022, Article ID 5719525, 11 pages
https://doi.org/10.1155/2022/5719525

Research Article

Characterization of Urban Bus Acceleration Cycles for Fatigue Analysis with a Portable Low-Cost Acquisition System

JesusAngel Pérez,[1] **JoseLuis Olazagoitia**,[2] **and Francisco Badea**[2]

[1]*Department of Construction and Manufacturing Engineering, Mechanical Engineering Area, University of Oviedo, 3394 Gijón, Spain*
[2]*Department of Industrial Engineering and Automotive, Nebrija University, Pirineos 55, 28040 Madrid, Spain*

Correspondence should be addressed to JoseLuis Olazagoitia; jolazago@nebrija.es

Received 4 October 2021; Accepted 25 February 2022; Published 22 March 2022

Academic Editor: Cong-Bin Fan

The fatigue design of bus structures is directly dependent on the loads that the vehicle will support throughout its lifespan. The determination of such operational loads, obtained in form of accelerations through vehicle sensing, is usually done with proprietary and expensive acquisition systems. In this paper, a low-cost acquisition system is presented and studied, which is designed, calibrated, and oriented for this purpose, based on an Arduino UNO and a low-cost accelerometer. The acquisitions are adapted to obtain the operational loads of several urban bus lines in the city of Madrid. The obtained data is later processed in order to characterize the acceleration cycles in these structures, which can be used as an input for the appropriate structural design. As a result, it is proved that the low-cost acquisition system is adequate and provides a simple and cheap way to characterize the acceleration of these vehicles during ordinary service.

1. Introduction

There is a constant necessity for real-time data acquisition for both industrial and research development. In the particular case of transportation by buses and coaches, the acceleration characterization during normal driving conditions presents a significant interest for the structural design and improvement (fatigue, weight reduction, etc.), study of comfort aspects for both passengers and drivers, or even for the analysis of driving habits for the improvement of training programs at a much subtle level.

Bus and coach structures, together with their integrated systems, are subjected to time-varying loads that rise from the accelerations that this type of vehicle withstands during operation. As such, fatigue takes special relevance as one of the most common failure modes, and thus, an accurate characterization of the fatigue loads becomes of major interest for a proper structural design in terms of fatigue resistance.

In general terms, fatigue design of complex structures, as is the case of bus and coach bodies, is a challenging process in which multiple aspects ranging from the structural characteristics, loads, material properties, etc., must be taken into consideration. For example, in the case of the railway industry and most specifically in the design and fabrication of high-speed trains, fatigue plays a fundamental role, being one of the main safety concerns, since fatigue failures during high-speed operation would lead to catastrophic consequences. The structural design of such vehicles is regulated in the European Union by the Standard EN 12663 [1], which represents one of the most advanced regulations of its kind worldwide. For the evaluation of the fatigue, the normative provides a series of representative accelerations per direction, which have been obtained by analyzing historical data on multiple trains all over Europe.

For fatigue evaluation, the designer must obtain a detailed finite element method (FEM) model of the structure taking into consideration the structural characteristics along with the mass and general mass distribution of the vehicle. From this model, all possible combinations for the commented accelerations per direction must be considered input loads, together with the proper restriction points. The FEM model will output an accurate estimation of the stresses

acting on the structure for each simulated acceleration combination.

Analyzing the stress results from these simulations, correct fatigue assessments can be done by means of S-N diagrams (Wöhler curves), cumulative damage by Palmgren-Miner rule, Goodman criterion, etc. In the particular situation of the EN12663 standard, if infinite life is to be proven, all points of the model must show stress amplitudes that correspond to endurance of at least 10^7, which is considered the fatigue limit.

Unfortunately, a similar reservoir of input data is not available for the fatigue evaluation of bus and coach structures. This fact motivated the authors to explore a feasible manner for the characterization of such representative accelerations utilizing a customized low-cost acquisition system.

Nevertheless, the collection of data and operating loads of urban buses is usually time-consuming and requires specialized and expensive equipment. It is common to perform tests and trials on special test tracks designed for this purpose [2]. From these data, it is possible to obtain a fatigue load spectrum for accelerated durability testing, such as the one presented in [3] for tractor front axles. However, it would be desirable to be able to acquire these data with low-cost equipment, without the need to access specialized test tracks, so that actual service loads can be recorded.

In the relevant literature, it is possible to find works that use low-cost methods for data acquisition. For example, in [4], a general, low-frequency acquisition system in environmental applications was presented. In vehicles, in [5, 6], some systems that allow acquiring these accelerations are introduced. On the one hand, in [5], vehicle accelerations are acquired and analyzed to evaluate the conditions of the vehicle driver. In [7, 8], a classification of a driver's driving style based on long-term accelerometer information is similarly performed. On the other hand, in [6], data are acquired to detect vehicle maneuvers, classifying the acquired accelerations. In [9], these accelerations are used to evaluate the comfort of commuters in public transport, based on dynamic acquisition and relying on passenger feedback. In [8], a low-cost prototype for vehicle behavior identification and vehicle fault detection is discussed.

In [10], it was already demonstrated that it was possible to use low-cost acquisition systems for dynamic applications. In that paper, professional accelerometers were compared with low-cost ones, and it was concluded that they could be used satisfactorily.

Another low-cost alternative for data acquisition in vehicles is provided by sensors integrated into smartphones. For example, in [11], the acquisitions obtained from the sensors of a smartphone to identify the mode of transport used by the user are analyzed. In this case, the acquisitions depend on the specific software used, not allowing additional programming.

Acquisition of acceleration data in vehicles is a common practice. However, there are not many applications in which low-cost acquisition systems are used in passenger vehicles, and when they are used, they are focused on the detection of driver maneuvers, either to know their status or to know their impact on passengers. Besides, as far as data acquisition for component fatigue monitoring is concerned, applications are usually focused on the study of the fatigue state of a specific component, such as automotive coil springs [12], the detection of fatigue in components in naturalistic driving environments, or the determination of the nonlinear characteristics of a passenger vehicle suspension [13].

Following a review of the relevant literature, it was found that there is a lack of low-cost acquisition systems for acceleration data acquisition aimed at obtaining the acceleration cycles to which a passenger bus is subjected during normal operation. These cycles are of utmost importance for the overall design of bus and coaches, and unlike the case of the railway industry introduced above, there is no standardized procedure or information. Rather, manufacturers prefer to keep it confidential as know-how for the design of better vehicles.

In this paper, it is presented the configuration, design, development, and acquisition of actual acceleration data on passenger buses in different transport lines in the city of Madrid. The developed system is characterized for being low cost, unobtrusive, and easy to handle, with a proven suitable acquisition frequency of about 100 Hz, a minimum autonomy of 3 hours running with easily replaceable batteries, and high stability and reliability.

In all, 10 routes were successfully recorded with the acquisition system. The data was later processed to characterize the acceleration loads during normal operation with the ultimate objective to extract the acceleration cycles to which they are subjected.

Fatigue assessments are performed in terms of load cycles (i.e., closed-loop load reversals), which are then compared to the material strength databases to predict fatigue damage and failure. The extraction of such cycles from complex time histories, as is the case of bus acceleration loads, is not straightforward. A series of cycle counting algorithms have been proposed over the last decades [14], of which one of the most well-known and accepted is the so-called rainflow cycle counting method [15], developed by Endō and Murakami. This method is employed in the present article to extract the acceleration cycles from the recorded data, which can be directly used as an input in any bus structure computational model, properly defined with its corresponding geometry, mass, and material characteristics, to determine the consequent fatigue stress cycles on the structure. It should be pointed out that the use of this data is limited to the bus structure itself, not to the vehicle components or systems and its supports, which would require specific analysis to account for its particular operating characteristics, as stated in [1]. For improved clarity, the integration and processing of the acceleration cycles obtained in the present work in the fatigue design process of bus structures are introduced in Section 6.

The novelty of the article resides in the development and testing of a low-cost acquisition system, which is accurate and stable, to acquire dynamic data from passenger vehicles and determine vehicle operating accelerations, presented as a viable alternative to commercial acquisition systems and extendable to any vehicle or machine undergoing accelerations of similar ranges and frequencies. In addition, the

results of the article provide a characterization of the bus transport operating accelerations, as well as the actual fatigue cycles that they have to withstand. This data supposes valuable information, which is of great use for the structural and fatigue design of this type of vehicle and is difficult to obtain at a low cost.

2. Low-Cost Acquisition System Description

The primary goal of the acquisition system is to record a representative sample of the accelerations of urban transport busses during normal operation. This measuring scenario generates several design restrictions of the acquisition system. Firstly, accelerations should be measured during bus ordinary transit routes. This compels to construct a nonintrusive system which has no impact on the operation of the bus. Secondly, it was necessary to use a discreet system that does not disturb or attract the passenger's attention, so the device should be small enough to be easily hidden during the measuring time. Thirdly, the acquisition system needs to be standalone and portable to allow easy switching from one bus to another and thus obtain acceleration data from different routes. Finally, the acquisition system must be stable over the relatively long duration of the measuring time, which corresponds to the duration of a complete bus route (40-50 minutes). During this time, the data cannot show any kind of drift or distortion.

To comply with these requirements, a customized Arduino-based acquisition system was designed and constructed composed of the following components:

(1) *MMA7361 Triaxial Accelerometer*. The capacitive micromachined accelerometer acquires the acceleration data and sends it to the processor unit in form of millivolts. Its main characteristics are shown in Table 1. This accelerometer offers the possibility to choose between two measuring ranges, ±6g and ±1.5g. Given the nature of the vehicles to be measured, exceeding 1.5g of acceleration during operation would be a very rare situation that would most probably lead to instabilities or even accidents due to the dynamic limitations of these vehicles governed by adherence to the road. For this reason and with the purpose of increasing the sensitivity, a measuring range of ±1.5g was selected. Equipment and equivalent procedure presented in [10] were followed to calibrate the accelerometer sensor. Calibration data obtained with respect to the reference accelerometer Brüel Type 4534-B are summarized in Table 2.

(2) *4-Gigabyte Micro SD Card*. The 4-gigabyte micro SD card stores the acceleration data. It was verified that more than 600 hours of accelerations can be stored at a sampling rate of 100 Hz in such capacity, which supposes way more than the target measuring time of 8 hours of operation.

Table 1: MMA7361 accelerometer characteristics.

Characteristic	Value
Operating current	400 μA
Operating voltage	2.2-3.6 V
Operating temperature	-40-85°C
Measuring range[1]	±1.5g
Bandwidth response	300 Hz (Z)–400 Hz (X, Y)
Output voltage[1]	0-3.3 V
Sensitivity[1]	0.8 V/g

[1]With high sensitivity selected.

Table 2: Calibration data utilizing Brüel Type 4534-B accelerometer as reference, up to 100 Hz.

Accelerometer	1 Hz	5 Hz	10 Hz	25 Hz	50 Hz	100 Hz
MMA7361	1.52%	1.55%	1.68%	1.72%	1.65%	1.54%

(3) *Arduino UNO Microcontroller*. It controls the acquisition process. When the trigger button is pressed, it starts acquiring accelerations, converting them to a digital signal through the 10-bit resolution ADC converter, and sending them to the storage unit. When the trigger button is pressed for the second time, the acquisition process stops. The microcontroller also supplies the necessary power to the accelerometer and the SD card. The relevant features of the microcontroller are summarized in Table 3.

(4) *9-Volt Alkaline Battery*. The 9-volt alkaline battery supplies the power to the microcontroller, which then distributes to the accelerometer and storage unit. The batteries used were tested to supply stable power for around 3 hours. It was decided to replace it every 2 routes (80-100 minutes).

Given the resolution of the microcontroller and the sensitivity of the accelerometer, the minimum acceleration change that can be detected results in $0.0032/0.8 = 0.004$g or $0.0395\ \text{m/s}^2$. The wiring diagram of the acquisition system is shown in Figure 1.

With respect to the sampling rate, relevant literature shows that the most significant loads arising from pavement irregularities range from 0.5 Hz to 50 Hz [16]. Furthermore, the damping effect of the suspension system absorbs frequencies from 10 to 15 Hz, depending on the working conditions and suspension design [17, 18]. It is therefore usual to find literature where acceleration signals are filtered out from frequencies of 20-25 Hz or even up to 2 Hz when the study focuses on horizontal accelerations [17, 19, 20]. For the present work, a sampling frequency of 100 Hz was used, which was proven to record all relevant acceleration events, as will be introduced in the following section.

Regarding the placement of the accelerometer within the buses, it was successfully validated that the car body can be

Table 3: Arduino UNO features.

Characteristic	Value
Supply voltage	7-12 V
Processor	Atmega 328
Clock frequency	16 MHz
Flash memory	32 kB
Analog input pins	6
Digital I/O pins	14 (6 provide PWD output)
ADC converter	10 bits
Analog signal range[1]	0 V to 3.3 V
Analog signal resolution[1]	0.0032 V

[1]Reference voltage 3.3 V selected, in accordance with accelerometer output voltage.

considered a rigid sprung mass for dynamic behavior modeling [18]. It is thus common practice to base these measurements on one accelerometer usually installed on the bus floor [19–21]. On these bases, the acquisition system was fixed to the bus floor using a cyanoacrylate high-performance adhesive. The attachment surfaces were previously cleaned to remove dirt particles that might mitigate the performance of the adhesive compound.

3. Data Stability Assessment

Since the acquisition system should be recording acceleration data continuously in a complete bus route, the signal should be stable and show no significant drift during this time, which could bias the results. In order to assess this, the acquisition system was set to acquire in a steady state over close to 45 minutes, which corresponds to the average route duration. The obtained mean and standard deviation in each measuring direction are shown in Table 4. Also, an extract of the time history of the accelerations is shown in Figure 2. For clarity and given the high similarity among the three directions, only the last minute of Z accelerations is shown. It is noted that the average values obtained for the three acceleration directions are almost zero. Also, the time history shows how the signal remains zero-centered after 40 minutes of steady measurements (i.e., no drift is observed). To ensure such stability on the data, it was proven the necessity to employ high-quality batteries that provide stable power to the Arduino microcontroller. In any case, a little measuring time in a steady state before and after every bus route was performed in order to confirm that the signals remained without drift. In this situation, though, accelerations before and after might slightly differ due to differences in the road characteristics at the beginning and at the end of the route in terms of slope, cant, etc.

When a perfect, noiseless acquisition system measures in a steady state, no accelerations at all should be recorded. Any deviation in this situation is due to noise, which can be quantified by the dispersion of the data.

In this case, in Figure 2, it can be observed that the acceleration acquisitions show a range of 9 discreet steps, each corresponding to the resolution of the system (0.0395 m/s^2). It indicates that the noise range during 1 minute of measurement is already 9 times higher than the resolution of the acquisition system. In consequence, an improvement of the resolution itself would not have a significant impact on the quality of the signal. In any case, as will be shown later, the noise is around one order of magnitude lower than the actual accelerations during bus operation, so the signal was considered acceptable for the purpose of this work. Moreover, the signal filtering performed will further reduce the influence of the noise.

4. Data Acquisition and Signal Filtering

With the purpose of collecting representative data to characterize bus accelerations, a total of 10 routes belonging to 5 different lines were recorded. Every line was measured for both its outward and return routes.

The main characteristics of these lines are summarized in Table 5. The selection was made on the basis of measuring lines with diverse features in order to obtain acceleration data from a wide range of operating conditions.

In all, around 8 hours of longitudinal, lateral, and vertical accelerations during ordinary bus service were recorded. The battery was replaced every line change (i.e., two routes) to ensure no data biasing due to running out of power. The accelerometer was placed in the busses in such a way that X acceleration corresponded to the longitudinal moving direction, Y acceleration with the lateral direction, and Z acceleration with the vertical direction.

To reduce the influence of noise in the results as much as possible, the acceleration data was filtered using a 6th-order low-pass Butterworth filter. This type of filter leaves unchanged the data for lower frequency and applies a progressive response decay in a way that for the established cutoff frequency, the response of the filter is $1/\sqrt{2}$. It is then important to establish a proper cutoff frequency that minimizes the noise influence without eliminating actual acceleration information.

It should be also considered that the source of the accelerations differs depending on the direction: whereas the longitudinal and lateral accelerations are mainly originated from driving maneuvers, the vertical ones arise from road imperfections. Consequently, they cannot be supposed to occur at the same frequencies, and therefore, cutoff frequencies should be established independently.

To determine the adequate cutoff frequencies, discrete Fourier transforms (DFT) of actual acceleration data were compared with the stationary measurements recorded as described in the previous chapter. Figure 3 shows the superposition of the amplitudes of both data (upper side graphs) and the difference between them (lower side graphs) for the three acceleration directions. It is observed that most significant acceleration amplitudes occur at lower frequencies. It is also noted specially for vertical accelerations and also for lateral and longitudinal ones, an amplitude peak in the range of 2-3 Hz, most probably originated by the natural frequency of the bus sprung mass. From this frequency range, amplitudes decrease for longitudinal and lateral accelerations, becoming their differences with the stationary data almost neglectable from 5 to 7 Hz. In the case of vertical acceleration, some minor differences can be observed up to 10-15 Hz.

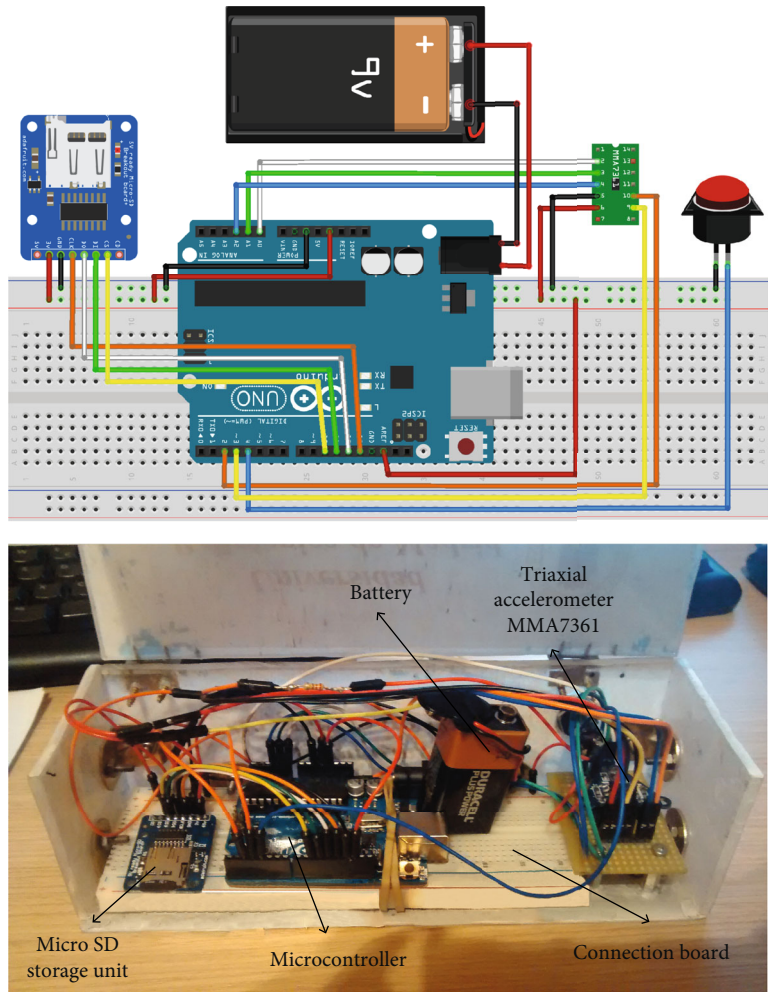

Figure 1: Acquisition system layout and actual assembly.

Table 4: Mean and standard deviation of steady-state acceleration data.

	X acceleration	Y acceleration	Z acceleration
Average (m/s^2)	-0.00004	-0.00007	-0.00005
Std. dev. (m/s^2)	0.0568	0.0541	0.0498

Based on these observations, conservative cutoff frequencies of 10 Hz for X and Y accelerations and 20 Hz for Z accelerations were adopted. The resulting filtered data in the frequency domain are shown in Figure 4, where it is clearly seen that the significant acceleration amplitudes remain unaffected, whereas noisy amplitudes that occur at higher frequencies are removed from the signal.

The characterization of the accelerations presented in the following section is based on the obtained filtered data.

5. Results

5.1. Urban Bus Acceleration Characterization. The acceleration events arise from the normal bus operation. Therefore, when the bus is at a full stop, only noise and vibrations are recorded, which are irrelevant for the fatigue assessment of the bus structure. For this reason, idling periods belonging to bus stops, traffic lights, and the initial and final stationary measuring periods were removed from the analysis. By way of example, Figure 5 shows the acceleration data recorded from one of the routes of line 21, where the idling periods are highlighted in red. Some aspects can be noted from the observation of this graph. It is first observed that the highest acceleration values occur in a vertical direction (Z). Nevertheless, due to the source of these accelerations, the recordings are dominated by almost zero values corresponding to circulations through stretches in good condition, in which significant amplitude accelerations intercalate when the bus passes through bumps or road imperfections. Consequently, as will be shown later in this section, the overall standard deviation of these accelerations is smaller than that in the X direction.

Also, there seems to be some correspondence between vertical and lateral accelerations, although the latter is in a minor range, most likely originated because of the influence of road imperfections on the lateral accelerations. This influence is not observed in the X direction.

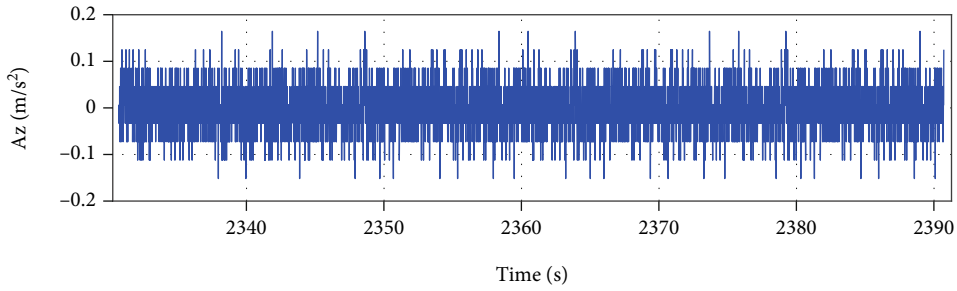

Figure 2: Last minute of steady-state acquisition of vertical accelerations.

Table 5: Selected bus line characteristics.

Line	Number of stops[1]	Route distance[1] (km)	Average speed[1] (km/h)
15	19	6.24	11.44
21	35	9.21	10.91
63	27	11.61	17.07
71	42	12.72	14.34
140	30	8.75	12.87

[1]Per route.

The idling periods (i.e., when the bus is completely stopped) do not always correspond to zero-centered values for X and Y accelerations, which are sensitive to bus stops in zones with slope and cant, respectively. The Z direction, which is much less sensitive to this effect for small inclination angles, remains zero-centered along the complete route, which indicates no drift on the signal.

Longitudinal accelerations seem to repeat a pattern between stops, with an initiation bus acceleration peak ($X-$), followed by a progressive decrease, sometimes with a flat and close to zero acceleration period (constant velocity), and finally a deceleration peak ($X+$) just before the next stopping period. This pattern shows clear correspondence with bus operation in which, after a stop, the bus accelerates up to a certain speed, depending on the traffic conditions, maintains near-constant speed for some time, and finally brakes the bus to a new stop.

The overall acceleration frequency distributions after removing the idling periods are shown on the histograms of Figure 6. Although some events beyond the graph's limits were registered, the histogram plots were set between $\pm 2\,\mathrm{m/s^2}$ for greater clarity. The mean and standard deviation of the samples correspond to the totality of the recordings. As it was previously advanced, the maximum number of events close to zero corresponds to vertical accelerations and the minimum, by far, to the longitudinal ones. This indicates that longitudinal accelerating/braking events are relatively more frequent than passing through curves or canted roads (lateral) or road imperfections (vertical). Average values are almost zero in all cases and the distributions close to symmetrical, except for longitudinal accelerations, where a slight asymmetry can be observed, probably due to the characteristics of the acceleration—brake pattern observed.

Finally, it is noted that the standard deviations of actual acceleration recordings are almost one order of magnitude higher than the ones from the steady-state measurements shown in Section 3, even unfiltered. They are therefore considered adequate for the current purpose of bus acceleration characterization.

Table 6 shows the upper and lower bound percentiles obtained from all acceleration data. In accordance with the previous observations, it is noted that the X direction shows higher acceleration values than the Y and Z directions for the less extreme percentiles P_5 and P_{95}. This behavior changes already for percentiles P_1 and P_{99}, where the Z direction becomes the direction with the highest recordings, while X and Y directions show almost the same values. For the most extreme percentiles $P_{0.1}$ and $P_{99.9}$, the Z direction clearly shows the most significant accelerations, and the tendency inverts for the X direction, being now the direction that presents the lowest values.

From the results, it can be concluded that most frequent normal operation is led by longitudinal accelerations and that less frequent events arise from passing through curved roads, and specially through road imperfection and bumps, it shows the highest acceleration values on the buses. In any case, it should be noted that all the recordings are well below the dynamic limits of these types of vehicles.

5.2. Fatigue Load Results. Although one might be tempted to construct acceleration cycles based on the frequencies presented above, for example (P_5, P_{95}), it would not be technically correct for fatigue design, since such cycles might not exist, or even if they do, they will not be the only ones that can induce fatigue damage. Thus, to obtain proper acceleration cycles that buses suffer during operation, a cycle extraction method needs to be used. In this case, the widely used and accepted rainflow counting technique [15] will be employed. The algorithm extracts closed loading reversals (i.e., cycles) from the time series as illustrated in the example of Figure 7. It evaluates two load ranges every three consecutive points (B-C and C-D in the example). If the first range is smaller than the second range in absolute terms ($|C\text{-}B| < |D\text{-}C|$), a cycle is located, and the corresponding average (a_{avg}) and alternate (a_{alt}) components are determined. The algorithm continues by removing points B and C from the time series and restarting the process from point A. It will repeat this process until all points are removed,

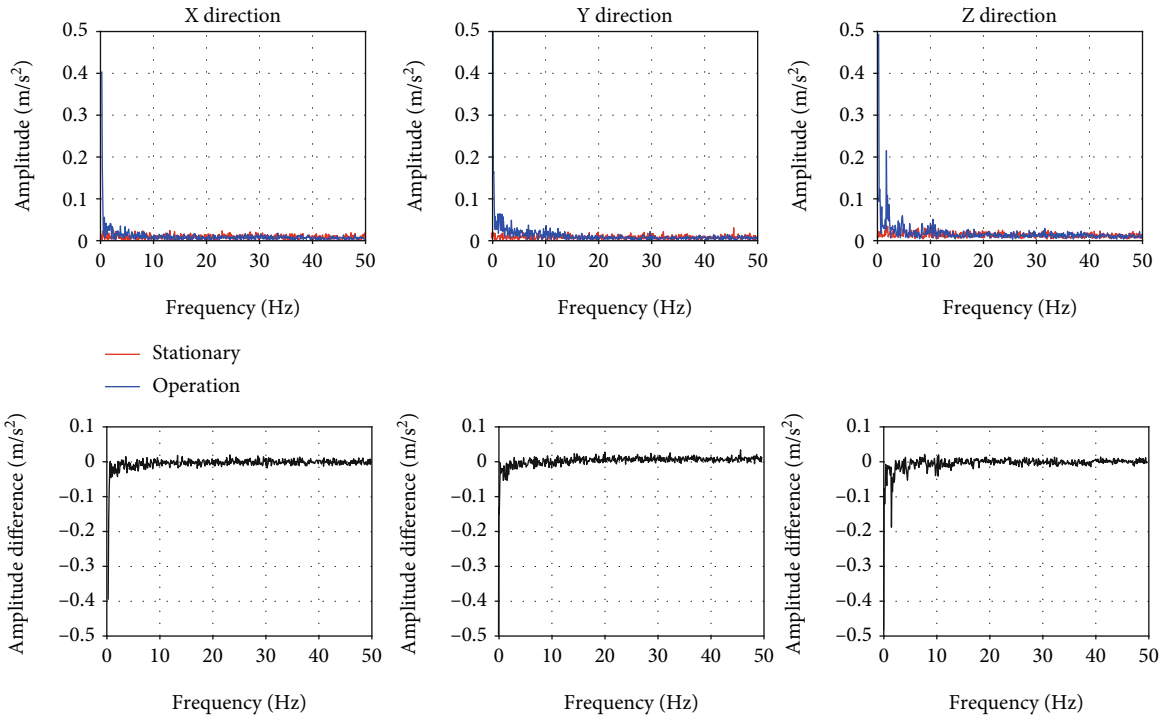

Figure 3: Frequency response comparison between steady-state and operation accelerations.

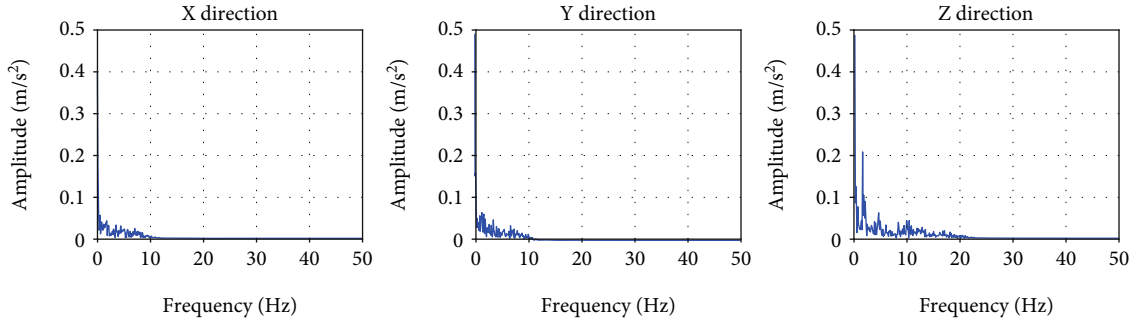

Figure 4: Resulting frequency response of filtered acceleration data.

meaning that all existing cycles have been extracted from the time series.

Every acceleration cycle is fully defined by its average value (a_{avg}) around which the alternate component oscillates (a_{alt}). They can therefore be arranged in matrix form for different classes of (a_{avg}, a_{alt}), for which the number of cycles located in every class is accounted. Such arrangement is shown in Figure 8 and the corresponding matrices of Table 7 divided into classes of range $\pm 1\,m/s^2$. In this figure, the Z axis has been limited to 30000 events for visual clarity purposes. Similarly to the behavior observed in the histograms of Figure 6, X accelerations show the least $(0, 0)$ -centered cycles and also the smallest amplitude cycles in comparison to X and Y accelerations. It is also noticed, especially for the X and Y directions, that the highest acceleration amplitudes arise at low average values, and vice versa. This fact goes in accordance with the normal driving style, in which performing significant turnings when already in a curve or a sharp brake during an already significant breaking or accelerating maneuver is not a very logic operation, which might be performed in case of emergency situations and could lead to vehicle instability or even accidents. This observation is not so clear for Z accelerations, which, as introduced before, do not arise from driving maneuvers controlled by the driver but from bumps and road imperfections. In this direction, the average accelerations seem to be slightly uncentered, probably due to the damping effect of the vehicle suspension.

The acceleration cycles here obtained can be directly used as an input in any structural design model to assess its fatigue behavior. For the sake of clarity, the integration of this data into the fatigue design of a bus structure is presented in the following section. It should be noted that these cycles correspond to about 8 hours of operations, and thus, the total number of cycles that the structure will actually withstand should be calculated from extrapolation to the lifespan of the vehicle considered by the manufacturer.

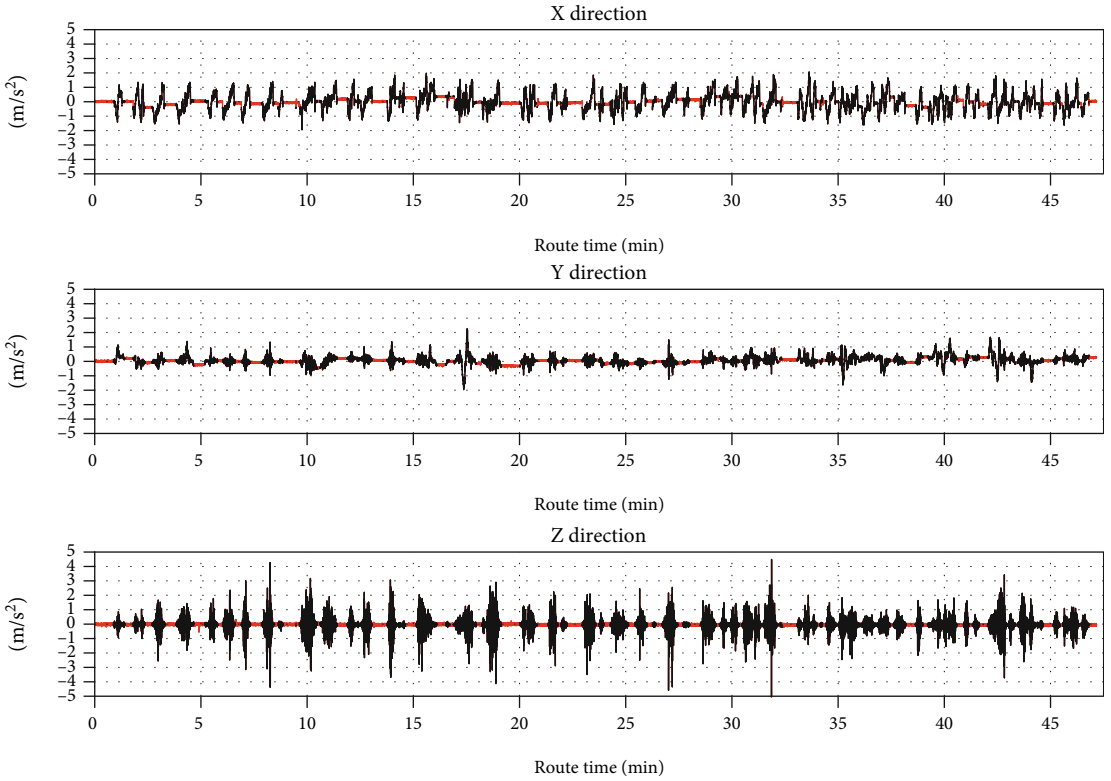

Figure 5: Line 21—acceleration data.

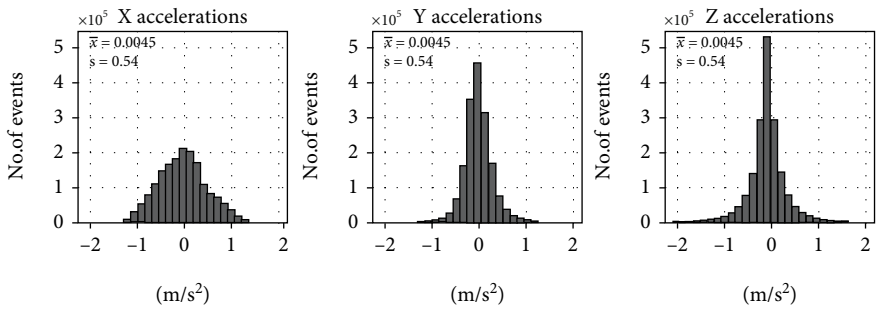

Figure 6: Acceleration frequency distributions.

Table 6: Bus acceleration percentiles.

Percentile	X acceleration (m/s^2)	Y acceleration (m/s^2)	Z acceleration (m/s^2)
$P_{0.1}$	-1.41	-1.81	-2.87
P_1	-1.14	-1.14	-1.38
P_5	-0.86	-0.52	-0.66
P_{95}	0.95	0.60	0.66
P_{99}	1.28	1.16	1.35
$P_{99.9}$	1.67	1.88	2.77

6. Procedure for Fatigue Evaluation

The implementation of the obtained results in a complete fatigue assessment for a typical bus structure design based on the finite element method (FEM) is shown in the schema of Figure 9. Although some minor modifications might be encountered in the literature, the basic design flow shown in the figure is a standard practice in the modern industry. Also, relying in computer-aided engineering techniques such as FEM is very extended, and there are numerous commercial packages suitable for running calculations of bus structures.

Starting from an initial structural design proposal, which completely defines the geometry and the material characteristics of the structure, a FEM model is constructed. During this process, the model is divided into a small, simple-shaped, and finite number of elements, which have the material information associated. Then, the acceleration cycles obtained in the last section are input as inertial loads. The model must also be properly restricted at the points of interaction with the suspension system. With all this information

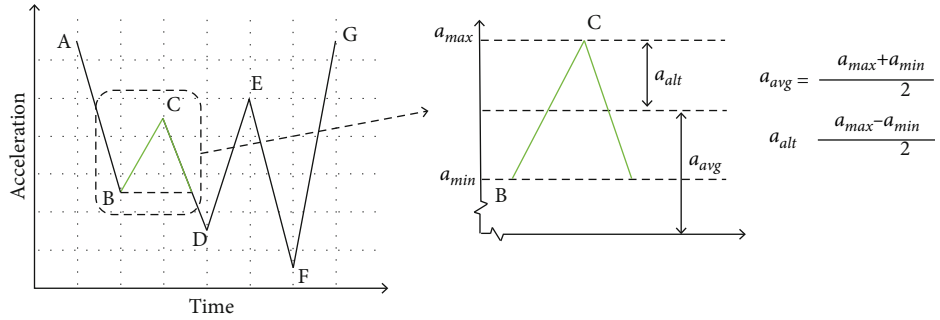

Figure 7: Schema of cycle extracting process with rainflow method.

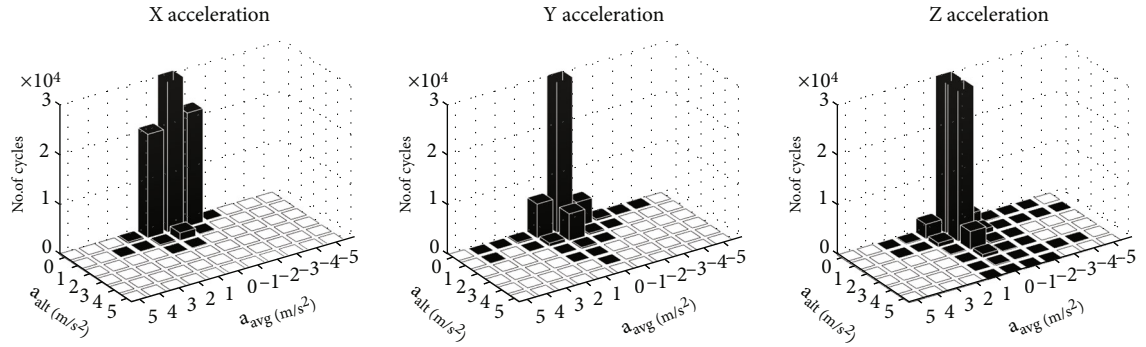

Figure 8: Acceleration cycle graphs.

Table 7: Acceleration fatigue cycle table.

a_{avg} (m/s^2)	X acceleration a_{alt} (m/s^2)						Y acceleration a_{alt} (m/s^2)						Z acceleration a_{alt} (m/s^2)					
	0	1	2	3	4	5	0	1	2	3	4	5	0	1	2	3	4	5
-5	0	0	0	0	0	0	0	0	0	0	0	0	0	**2**	0	0	0	0
-4	0	0	0	0	0	0	**1**	0	0	0	0	0	**9**	**2**	0	0	1	0
-3	0	0	0	0	0	0	**1**	0	0	0	0	0	**18**	**3**	0	0	1	0
-2	**36**	0	0	0	0	0	**300**	**12**	0	0	0	0	**96**	**8**	**1**	**4**	**2**	**3**
-1	**22*E*3**	**62**	0	0	0	0	**4794**	**237**	**8**	0	0	0	**2429**	**885**	**218**	**92**	**49**	**19**
0	**86*E*3**	**1410**	**57**	0	0	0	**13*E*4**	**5279**	**212**	**28**	**7**	0	**19*E*4**	**34*E*3**	**3530**	**588**	**130**	**36**
1	**21*E*3**	**198**	**1**	0	0	0	**6734**	**570**	**21**	**6**	0	0	**2815**	**716**	**117**	**43**	**12**	**1**
2	**249**	**1**	0	0	0	0	**204**	**23**	0	0	0	0	**109**	**20**	0	0	0	0
3	0	**1**	0	0	0	0	**5**	0	0	0	0	0	**19**	**1**	0	0	0	0
4	0	0	0	0	0	0	**7**	**1**	0	0	0	0	0	0	0	0	0	0
5	0	0	0	0	0	0	0	0	0	0	0	0	0	0	0	0	0	0

set, the model is completely configured and ready to calculate the response of the structural design. Once the calculation is finished, the resulting stress cycles in response to the input acceleration cycles at each element of the model can be extracted.

Finally, the obtained stresses need to be processed to perform the fatigue evaluation based on any of the numerous available approaches (i.e., Goodman, Soderberg, and Palmgren-Miner). Usual outputs from fatigue assessments are the risk of fatigue failure in terms of fatigue safety factors, or damage levels, related to each element of the model. With this information, the design team can decide whether the structural design is valid in terms of fatigue. In that case, the design process is finished. If a redesign is needed, geometry, material, or both will be modified, and a new calculation iteration begins.

The importance of having reliable input loads in such a design process is evident. Utilizing over- or underestimated

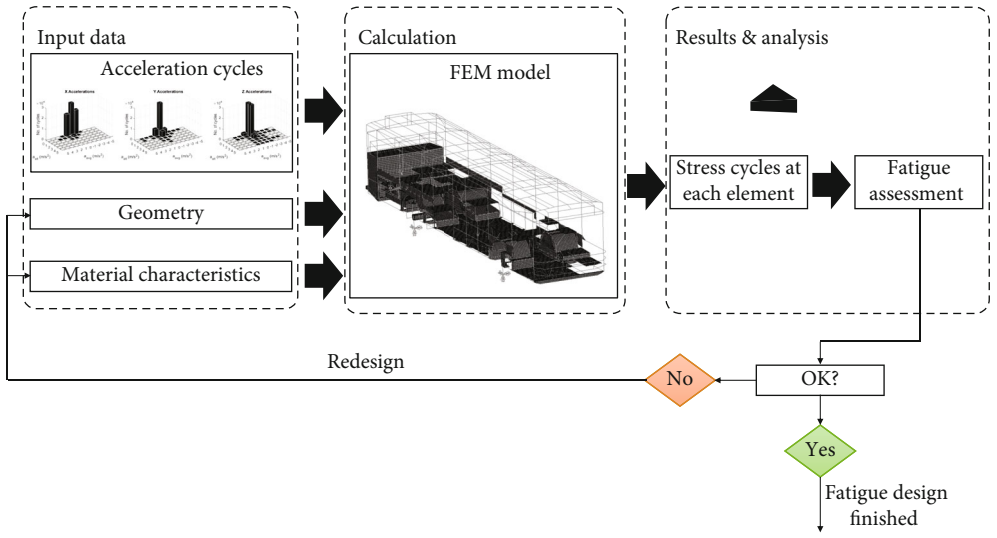

Figure 9: Acceleration cycle graphs.

input loads could lead, respectively, to overweighted designs, with the consequent effects on production costs and bus fuel consumption, or, even more dangerous, to a nonconservative design that might present unexpected fatigue failure during operation.

7. Conclusions

In the work presented in this article, a low-cost standalone acquisition system has been designed and built with the objective to measure acceleration cycles of urban buses during normal operation.

The acquisition system was proven to be stable along the relatively long measuring periods corresponding to complete bus routes. Also, accuracy and precision were verified to be adequate for the acceleration levels presented by these vehicles during normal operation.

A filtering procedure based on the comparison between noise, coming from steady-state recordings, and actual acceleration data was also applied, ensuring a proper selection of the cutoff frequencies without losing relevant information. It was shown that independent cutoff frequencies should be established for the different acceleration directions. In this case, 10 Hz was set for longitudinal and lateral accelerations and 20 Hz for the vertical ones.

In all, 10 different bus routes belonging to 5 different lines were measured, which supposed around 8 hours of acceleration data recordings in longitudinal (X), lateral (Y), and vertical (Z) directions. The measuring rate of 100 Hz was proved to be enough to capture all types of acceleration events regardless of the direction.

The acquired raw data was processed with the aim of characterizing the accelerations and extracting acceleration cycles. First, idling periods in which the bus is stopped were removed from the analysis, since no relevant acceleration events take place during this time. With the stopping periods removed, acceleration levels with respect to frequency of occurrence were obtained for the three directions. Some remarkable information was extracted from the analysis: on the on hand, it was observed that longitudinal acceleration histogram does not show a remarkable zero-centered density, such as in the case of lateral and vertical ones (Figure 7), meaning that during circulation, acceleration-braking periods are more common than passing through curves, cants, or road imperfections. On the other hand, extreme values recorded for lateral and especially for vertical acceleration levels are higher than that for longitudinal ones; this indicates that, although less frequent, lateral and vertical acceleration events can reach higher acceleration levels.

Finally, the acceleration time series was further processed to extract the acceleration cycles by means of the rainflow cycle counting method. Correspondence with logical driving maneuvers for X and Y accelerations was observed, since the most significant amplitude cycles corresponded in general to low average values and vice versa. Most significant fatigue cycles were extracted in the Z direction. In any case, the actual impact of these cycles in fatigue damage should be studied in conjunction with the response of the vehicle structure to them.

The application of the acceleration cycles obtained within the fatigue design of bus structures is detailed in Section 6. According to a typical design process summarized in Figure 9, these acceleration cycles are the input data to calculate the corresponding stress cycles at each element of a FEM model of the structure. With these stresses, any fatigue approach can be applied to assess the fatigue response at each element of the model. In this scenario, counting with reliable input information is crucial if optimized structural designs are to be obtained.

In conclusion, the data provided in this article yields valuable information about the solicitations withstood by urban buses during normal operation, with extensive application in fatigue structural design and analysis of bus body structures.

Data Availability

Data are included in the article, where relevant results are shown.

Conflicts of Interest

The authors declare that they have no conflicts of interest.

Acknowledgments

The authors thank the Global Nebrija-Santander Chair of Energy Recovery in Surface Transport for their financial support. This work was also supported by the Agencia Estatal de Investigación (grant RETOS 2018-RTI2018-095923-B-C22).

References

[1] UNE-EN 12663, "Railway applications - structural requirements of railway vehicle bodies," *European Norm*.

[2] M. Kepka, M. K. Miloslav Kepka, J. Václavík, and J. Chvojan, "Fatigue life of a bus structure in normal operation and in accelerated testing on special tracks," *Proceedings of the Procedia Structural Integrity*, vol. 17, pp. 44–50, 2019.

[3] C. Wen, B. Xie, Z. Li, Y. Yin, X. Zhao, and Z. Song, "Power density based fatigue load spectrum editing for accelerated durability testing for tractor front axles," *Biosystems Engineering*, vol. 200, pp. 73–88, 2020.

[4] D. K. Fisher and P. J. Gould, "Open-source hardware is a low-cost alternative for scientific instrumentation and research," *Mod (Instrumental)*, vol. 1, no. 2, pp. 8–20, 2012.

[5] T. Krotak and M. Simlova, "The analysis of the acceleration of the vehicle for assessing the condition of the driver," in *2012 IEEE Intelligent Vehicles Symposium*, pp. 571–576, Madrid, Spain, 2012.

[6] J. Cervantes-Villanueva, D. Carrillo-Zapata, F. Terroso-Saenz et al., "Vehicle maneuver detection with accelerometer-based classification," *Sensors*, vol. 16, p. 1618, 2016.

[7] V. Vaitkus, P. Lengvenis, and G. Zylius, "Driving style classification using long-term accelerometer information," in *2014 19th International Conference on Methods and Models in Automation and Robotics (MMAR)*, pp. 641–644, Miedzyzdroje, Poland, 2014.

[8] G. Andria, F. Attivissimo, A. Di Nisio, A. M. L. Lanzolla, and A. Pellegrino, "Development of an automotive data acquisition platform for analysis of driving behavior," *Measurement: Journal of the International Measurement Confederation*, vol. 93, pp. 278–287, 2016.

[9] J. C. Castellanos and F. Fruett, "Embedded system to evaluate the passenger comfort in public transportation based on dynamical vehicle behavior with user's feedback," *Measurement*, vol. 47, pp. 442–451, 2014.

[10] A. González, J. L. Olazagoitia, and J. Vinolas, "A low-cost data acquisition system for automobile dynamics applications," *Sensors*, vol. 18, no. 2, p. 366, 2018.

[11] A. Efthymiou, E. N. Barmpounakis, D. Efthymiou, and E. I. Vlahogianni, "Transportation mode detection from low-power smartphone sensors using tree-based ensembles," *Journal of Big Data Analytics in Transportation*, vol. 1, no. 1, pp. 57–69, 2019.

[12] D. Pastorcic, G. Vukelic, and Z. Bozic, "Coil spring failure and fatigue analysis," *Engineering Failure Analysis*, vol. 99, pp. 310–318, 2019.

[13] J. Sehovic, I. Filipovic, and B. Pikula, "Experimental determination of non-linear characteristics of the passenger vehicle suspension system," *Transactions of FAMENA*, vol. 44, pp. 13–22, 2020.

[14] Y.-L. Lee, J. Pan, R. Hathaway, and M. Barkey, *Fatigue testing and analysis: theory and practice*, vol. 13, Butterworth-Heinemann, 2005.

[15] T. Endō and Y. Murakami, *The rainflow method in fatigue : the Tatsuo Endo memorial volume, Butterworth-Heinemann*, vol. 1991, 1992.

[16] D. Sekulić and V. Dedović, "The effect of stiffness and damping of the suspension system elements on the optimisation of the vibrational behaviour of a bus," *International Journal for Traffic & Transport Engineering*, vol. 1, p. 4, 2011.

[17] F. Szauter, G. Istenes, and G. Rödönyi, "Spectral analysis of suspension system of a commercial city bus," in *2016 IEEE 14th International Symposium on Intelligent Systems and Informatics (SISY)*, pp. 67–72, Subotica, Serbia, 2016.

[18] T. Nguyen, P. Swolana, B. Lechner, and Y. D. Wong, "An experimental comparison of mathematical heavy-duty city bus models to evaluate passenger ride comfort induced by road roughness," *Mathematical and Computer Modelling of Dynamical Systems*, vol. 27, no. 1, pp. 203–221, 2021.

[19] M. Kirchner, P. Schubert, C. T. Haas, P. Schubert, and C. T. Haas, "Characterisation of real-world bus acceleration and deceleration signals," *Journal of Signal and Information Processing*, vol. 5, no. 1, pp. 8–13, 2014.

[20] A. Palacio, G. Tamburro, D. O'Neill, and C. K. Simms, "Non-collision injuries in urban buses–strategies for prevention," *Accident Analysis & Prevention*, vol. 41, no. 1, pp. 1–9, 2009.

[21] B. Jachimczyk, D. Dziak, J. Czapla, P. Damps, and W. Kulesza, "IoT on-board system for driving style assessment," *Sensors*, vol. 18, no. 4, p. 1233, 2018.